400178   UCRL-4505

Cy 3

UNIVERSITY OF CALIFORNIA

Radiation Laboratory, Livermore Site

Livermore, California

Contract No. W-7405-eng-48

SOME FISSION PRODUCT YIELDS OF URANIUM BOMBARDED WITH DEUTERONS OF VARIOUS ENERGIES (20-190 MEV)

Harry G. Hicks

Peter C. Stevenson

Richard S. Gilbert

William H. Hutchin

May 20, 1955

5001862

CONTENTS

<u>Illustrations</u>

SOME FISSION PRODUCT YIELDS OF URANIUM BOMBARDED WITH DEUTERONS OF VARIOUS ENERGIES (20-190 MEV)[*]

Harry G. Hicks

Peter C. Stevenson

Richard S. Gilbert[**]

William H. Hutchin

University of California Radiation Laboratory

Livermore Site

May 20, 1955

ABSTRACT

The formation cross sections of Sr^{89}, Zr^{97}, Pd^{109}, Pd^{112}, Ag^{111}, and Ba^{140} were measured from the bombardment of natural uranium with deuterons of various energies (20-190 Mev).

SOME FISSION PRODUCT YIELDS OF URANIUM BOMBARDED WITH DEUTERONS OF VARIOUS ENERGIES (20-190 MEV)

Harry G. Hicks, Peter C. Stevenson,

Richard S. Gilbert, and William H. Hutchin

University of California Radiation Laboratory

Livermore Site

May 20, 1955

I. INTRODUCTION

Lindner and Osborne[1] were among the first to study in detail the manner in which individual fission reactions change with bombarding particle energy in the hundred-Mev region. The present work furnishes additional data about individual fission reactions and serves to provide a somewhat broader basis for further study of the mechanism of high-energy fission.[2] Natural uranium was bombarded with various energy deuterons (20-190 Mev) and the following nuclides observed: Sr^{89}, Zr^{97}, Pd^{109}, Pd^{112}, Ag^{111}, and Ba^{140}.

II. EXPERIMENTAL PROCEDURE

Targets bombarded using the internal circulating beam of the Berkeley 184-inch cyclotron were assembled according to the schematic drawing in Fig. 1. The aluminum beam monitor and uranium target foils were sandwiched between guard foils of the same material to protect them from contamination and to compensate for loss of recoiling radionuclides. Foils were cut in a special device to produce foils of equal area. The monitor and target foils were weighed, assembled, and aligned to ensure that all foils intercepted the same beam intensity. Targets were bombarded

---

[1] M. Lindner and R. N. Osborne, Phys. Rev. 94, 1323 (1954)

[2] H. G. Hicks and R. S. Gilbert, UCRL-4506

of the observed nuclide. The maxima of the excitation functions in Fig. 2 are in general agreement with the previous observations. The decrease with increasing energy is ascribed to the increase of the formation probability of less neutron-rich isobars at the higher bombarding energies.[1]

The total 109 and 112 mass yields should be nearly the same, for these masses are near the expected peak of the high energy fission-product distribution. Below 75 Mev, the cross sections for formation of Pd^{109} and Pd^{112} are the same (Fig. 2), while above 75 Mev, the Pd^{112} (n/p = 1.44) formation cross section is lower than that of Pd^{109} (n/p = 1.37). This decrease of the Pd^{112} formation cross section relative to that of Pd^{109} can be attributed to the direct formation by fission of Ag^{112} (n/p = 1.38) by the above hypothesis. This effect was demonstrated by isolating a silver fraction from palladium a few minutes after a 190-Mev bombardment. This silver fraction was then purified from other fission products by standard radiochemical analyses. After correcting the observed Ag^{112} activity for growth from Pd^{112} before separation, the direct formation cross section was found to be 20 mb at 190 Mev. The difference between the Pd^{109} and Pd^{112} formation cross sections at 190 Mev was about 20 mb.

The Zr^{97} excitation function also shows a marked decrease with increasing energy (Fig. 2). Attempts were made to measure the direct formation cross section of Nb^{97}, but the niobium could not be separated from the zirconium present with sufficient rapidity to afford an unambiguous answer. After correction for the growth from Zr^{97}, the upper limit of the Nb^{97} cross section was set at 8 mb. The maximum of the Zr^{97} cross section is 78 mb, and the cross section at 190 Mev is 72 mb (Fig. 2). This decrease is just outside the experimental error and is almost certainly less than 8 mb. The results of the study of the 97 chain, while not conclusive, are in agreement with the postulate.

IV. ACKNOWLEDGMENTS

The disintegration rate of a sample was determined by the equation:

$$\text{disintegrations/min} = (\text{counts/min})_{Obs} \left(\frac{f_{aw}}{f_s}\right) \left(\frac{100}{g}\right) ,$$
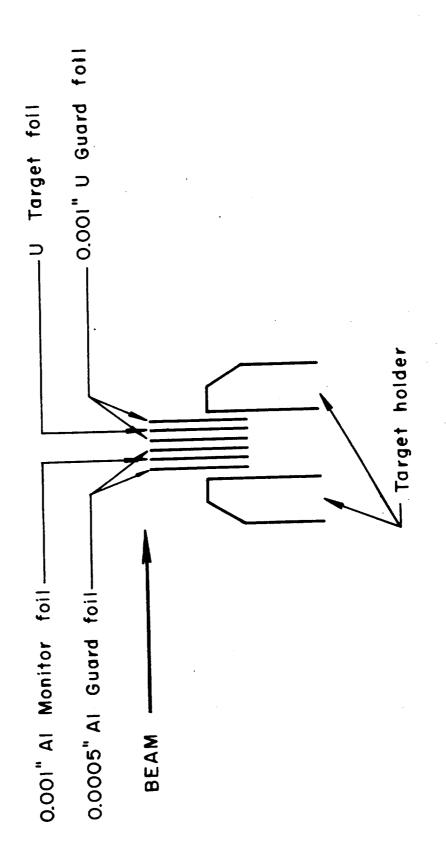
in which f_{aw} is the correction for air gap and window absorption, f_s, the total scattering factor as defined by the ordinates of Fig. 3, and g is the percent physical geometry for the counter (3.11 percent) as measured by a Radium D EF Standard or by the 100 percent geometry counter.

The following is a summary of the chemistry and counting techniques used for the nuclides included in the excitation functions of Fig. 2.

Sr^{89}: Initial separation was delayed for one week so that the 9.7-hour Sr^{91} could decay to undetectable levels in order to avoid interfering radioactivity of the 61-day Y^{91}. The Sr was separated with Ba as the nitrate, scavenged with $Fe(OH)_3$ using NH_3 gas, the Ba removed by repeated precipitation of $BaCrO_4$ from NH_4Ac solution (pH 5), and finally the precipitation of Sr as the carbonate.

Zr^{97}: Initial separation was performed immediately after bombardment since its precursors are presumed to be short. The zirconium was extracted into $0.4\underline{M}$ thenoyltrifluoroacetone (TTA) in benzene from $4\underline{M}$ HCl or HNO_3 after initial extraction of the aqueous phase by diisopropyl ketone. The TTA phase was washed three times with $4\underline{M}$ HNO_3, evaporated to dryness, and ignited to ZrO_2.

Pd^{109}, Pd^{112}: Separation of the Pd fraction was made about two hours after bombardment so that more than 99.9 percent of the 22-minute Pd^{111} could decay, and thus minimize the Ag^{111} contamination of the final Pd fraction. A correction was made for the activity of the 3.2-hour Ag^{112} daughter of Pd^{112}. The Pd was separated as the sulfide from $6\underline{N}$ HCl and as the dimethylglyoxime (DMG). Scavenges of $Fe(OH)_3$ and AgCl were used, and the Pd was placed onto a Dowex A-1 column (5×0.3 cm of 200 to 300 mesh) with dilute HCl. The column was washed with $0.1\underline{M}$ HCl and $1.5\underline{N}$ H_2SO_4, and the Pd eluted with $1\underline{N}$ NH_4OH. The

Fig. 1 Schematic arrangement of target and monitor foils

0.00I" U Guard foil

U Target foil

0.00I" Al Monitor foil

0.0005" Al Guard foil
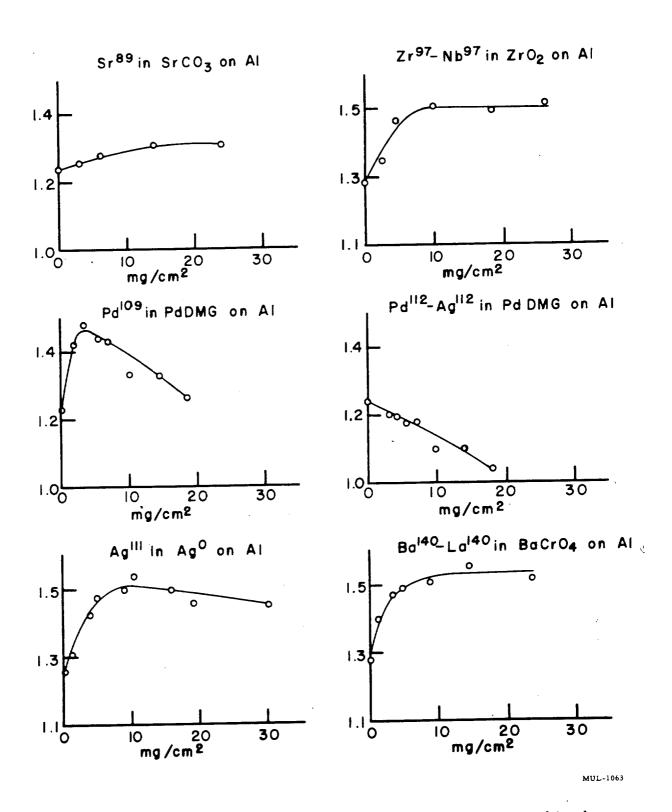
BEAM

Target holder

MUL-1061

Fig. 3. Empirical corrections of counting data for the combined effects of self-scattering, self-absorption, and saturation backscattering. The ordinates represent the ratio of observed counting rate to that of a carrier-free sample with the same disintegration rate mounted on a very thin backing (50 μg/cm²). The abscissae are the mass